ELSEVIER

Thermochimica Acta 385 (2002) 143–151

thermochimica acta

www.elsevier.com/locate/tca

Synthesis, reactivity, and cations inversion studies of nanocrystalline $MnFe_2O_4$ particles

N.S. Gajbhiye[*,1], G. Balaji

Department of Chemistry, Indian Institute of Technology, Kanpur 208016, UP, India

Received 9 March 2001; received in revised form 2 July 2001; accepted 17 August 2001

Abstract

Nanocrystalline $MnFe_2O_4$ particles were synthesized by using citrate precursor technique. Thermal decomposition of the precursor was studied by using TGA, DTG, DTA techniques. The decomposition products were characterized by gas and chemical analyses, IR, NMR, and XRD techniques. There are three major steps that involve in the decomposition process. The dehydration step, formation of intermediate acetonedicarboxylate complex and subsequent decomposition of acetonedicarboxylate to the stoichiometric, single phase $MnFe_2O_4$ at 350 °C with the evolution of H_2O, acetone, CO and CO_2 gases. The XRD crystallite size was found to be 7.0 nm and the surface area for this sample was measured to be 98.0 $m^2\,g^{-1}$. Electron micrographs confirmed the nanostructured nature, spherical morphology and showed 11 nm aggregates of particles. Thermal analysis studies of nanocrystalline $MnFe_2O_4$ particles indicate the higher degree of inversion and at 380 °C confirmed the irreversible rearrangement of Mn^{2+} cations from the octahedral site to tetrahedral site, that is associated with small a heat change.

Keywords: Citrate; Ferrite; Nanocrystalline; Precursor; Thermal decomposition

1. Introduction

The synthesis of magnetic nanocrystalline particles with controlled size and composition is of fundamental and technological interest. It was in the magnetic systems that the first finite size effects were observed [1–3]. Nanocrystalline materials are polycrystalline solids with grain size of a few nanometers. Because of large volume of fraction of interfaces, the electronic structure of nanocrystalline materials is likely to differ from one of perfect single crystals. This may lead to materials with modified overall physical properties when the scale of the microstructure is of the order of a few nanometers. Several reports document these significant effects of nanosize materials exhibiting size tunable properties and to build single electron devices [4–8]. However, the syntheses of spinel ferrites have been a long time technologically important to the microwave industries, high speed digital tapes and disc recording [9]. Therefore, the study of nanoscale magnetic domains is of prime interest since the advanced recording media is reducing rapidly to dimensions where magnetic properties strongly depend on nanocrystalline grain size. This has prompted to the development of various chemical methods that include hydrothermal, co-precipitation,

* Corresponding author. Fax: +91-512-590007.
E-mail addresses: nsg@iitk.ac.in (N.S. Gajbhiye), gbalaji@iitk.ac.in (G. Balaji).
[1] Presently Visiting Professor at the Institute of Nanotechnology, Forschungszentrum Karlsruhe, P.O. Box 3640, D-76021 Karlsruhe, Germany.

0040-6031/02/$ – see front matter
PII: S0040-6031(01)00714-6

freeze-drying and sol–gel for the preparation of stoichiometric and chemically pure spinel ferrites [10–14]. In our laboratory, citrate precursor technique has been shown to have great potential in the synthesis of rare earth iron garnets and some spinel ferrites [15–18].

Difficulties are encountered in the synthesis of nanocrystalline manganese iron ferrite particles as stoichiometric, pure phase and single domain nature [19]. The microstructure of the ferrite nanoparticles also depends on the synthetic method employed. There are no studies are available on the thermal decomposition of manganese iron citrate precursor. Therefore, we have investigated the synthesis of nanocrystalline $MnFe_2O_4$ through the control of solid state reactivity, during the thermal decomposition of citrate precursor, at low temperature.

2. Experimental

2.1. Reagents

The reagents: Mn metal was used from CDH, New Delhi, citric acid used was AnalaR grade S.D. fine Chem, Boisar, India. Ferric citrate used was GR grade from Loba Chemie, Bombay, India.

2.2. Preparation

Exact amount of manganese metal (0.5493 g) was weighed and dissolved in very dilute nitric acid and then diluted to 100 ml. An excess citric acid 0.2 M (80 ml) was added to make 200 ml of solution in water. To this solution, 0.2 M ferric citrate (100 ml) was added. Slightly excess citric acid was added to ensure efficient complex formation. The resultant homogeneous solution was refluxed in a 1 l capacity round-bottomed flask at 90 °C for 10 h in N_2 atmosphere to avoid oxidation of Mn^{2+} to Mn^{4+}. Finally, the solution was slowly evaporated on a water bath to form a viscous liquid and then transferred to a petri dish for drying at 100 °C in an oven for 5 h, to remove adsorbed water. During this process, the gel swells into a fluffy mass and breaks into brittle flakes. The degree of hydration (adsorbed water molecules) varied from 4 to 12 mol^{-1}. These flakes are then decomposed in an inert atmosphere.

2.3. Analysis

Manganese was estimated titrimetrically by persulfate–arsenite method [20]. Mn^{2+} is oxidized to permanganic acid by persulfate in the presence of silver nitrate solution as a catalyst. The permanganic acid is reduced by titrating with arsenite solution and the end point indicated by yellow color of the solution. Iron was estimated gravimetrically with 5% cupferron and subsequently weighed as Fe(III) oxide [20]. Chemical analysis by using atomic absorption spectroscopy was performed with a model AA-10, Varian, USA. The citrate content of the precursor and the intermediate products were estimated by using Karpov method [15,21]. The results of these quantitative analyses agreed well for the precursor, intermediates and the end products. During the decomposition, evolved acetone gas was tested by an iodoform test and a derivative with 2,4-dinitrophenylhydrazine. This was further confirmed by ^1H NMR spectroscopy using JEOL-PMX-60 S1, Japan. Quantitative analysis of acetone was performed by titrating excess acidified 0.1 M iodine solution against 0.1 M $Na_2S_2O_3$ solution in the presence of 1 M NaOH solution. A Perkin-Elmer 240C elemental analyzer was used to analyze the evolved gases. Thermal analyses (TG, DTG and DTA) of the citrate precursor were performed up to 700 °C by using simultaneous thermal analyzer system Mettler Toledo, Model-Star^e, Germany, in N_2 atmosphere at heating rate of 5 and 10 K min^{-1}. The samples were placed in a platinum crucible and ignited alumina was used as the reference material.

X-ray diffractograms were recorded using a Rich Seifert Isodebyflex X-ray unit model 2002 with Cu Kα radiation and Ni filter. IR spectra were recorded with a Perkin-Elmer model 377 IR spectrometer with a sample in the form of KBr pellets. Surface area measurements of the end products were obtained by the single point BET method with Coulter system model SA3100 using nitrogen gas as the adsorbate. The particle size and morphology were studied by using SEM, model JEOL-JSM-840A, and TEM, Philips model E-301.

3. Results

Wet chemical analysis of the manganese iron citrate precursor gave the amount of Mn: 7.6%, Fe: 15.1%,

Table 1
IR spectral frequency assignments for citric acid, ferric nitrate, precursor and different heat-treated products[a]

Citric acid	Ferric nitrate	Manganese nitrate	Precursor	Heat-treatment temperature (°C)			Assignments
				140	220	330	
3300 s	3700–3000 vs	3700–3000 vs	3700–3000 vs	3700–3300 vs	3700–3300 vs	–	ν OH water
3450 sh	–	–	3450 sh	3450 sh	–	–	ν OH hydroxyl
2900–2800 s	–	–	2900–2800 w	2900–2800 w	2900–2800 w	–	ν CH
1700 vs	–	–	1700 wsh	1700 wsh	1700 wsh	–	ν asym C=O
1620 w	1610 s	1600 s	1610 w	1610 w	–	–	δ HOH
–	–	–	1570 vs	1570 vs	1570 vs	–	ν asym COO
1430, 1385–1355 s	–	–	1400 vs	1400 vs	1400 vs	–	ν sym COO
–	1361 vs	1355 s	1361 vs	–	–	–	$\nu_3 NO_3^-$
1240–1190 s	–	–	1270 wsh	1270 wsh	–	–	ν sym CO
1080–1055 s	–	–	1080 br	1080 br	1080 br	–	ν st C–O
940–900 sh	–	–	940–900 sh	940–900 sh	–	–	Citrate
–	835 m	822 m	835 m	–	–	–	ν_2 NO_3^-
780 sh	–	–	780 sh	780 sh	–	–	Citrate
600–650 sh	–	–	600–650 sh	600–650 sh	–	–	Citrate
–	–	–	–	–	–	550 w	ν_1 $MnFe_2O_4$
–	–	–	–	–	–	392 m	ν_2 $MnFe_2O_4$

[a] s: strong; vs: very strong; sh: sharp; m: medium; w: weak; br: broad.

H_2O: 4.9% and citrate: 72.2% which agreed well with the values calculated for $Mn_3Fe_6O_4(C_6H_6O_7)_8{\cdot}6H_2O$, Mn: 7.5%, Fe: 15.2%, H_2O: 4.9% and citrate: 72.2%. The precursor adsorbs water depending on the humidity of the atmosphere. It was amorphous to X-rays. IR spectra of manganese iron citrate precursor, iron citrate, citric acid and ferric nitrate were analyzed and the results are shown in Table 1. The precursor has all the common bands of the citric acid and there are some bands that differ in their intensity and are broad in nature, which indicate the formation of hydrated citrate precursor. The broad bands in the region 3600–3000 cm^{-1} and around 1610 cm^{-1} could be due to the stretching and bending modes of water molecules because the intensity of these absorption decreases and disappears with the heat-treatment temperature. However, the broad band in the region 3229 cm^{-1} and the small shoulder at 1700 cm^{-1} could be attributed to the free hydroxyl and carboxylate group of manganese iron citrate. The broad and the unresolved bands at 1570 and 1400 cm^{-1} are characteristics of the completely ionized carboxyl group with equalized CO bands. A weak absorption near 1700 and 1385 cm^{-1} indicates some free citric acid. These studies indicate that the Fe- and Mn-ions are coordinated through carboxylate groups leaving free HO–C–COOH groups.

3.1. Thermal decomposition of the citrate precursor

TG and DTA curves were recorded for the precursor in flowing N_2 atmosphere with heating rate at 5 and 10 K min^{-1}. The representative TG and DTA curves are shown in Fig. 1. The complete data of the observed weight loss and the corresponding temperature ranges are given in Table 2. It can be seen that a one-to-one correlation exists between these thermoanalytical curves indicating that the thermal effects are accompanied by weight loss. There are three major steps in the decomposition process: dehydration, decomposition of the anhydrous precursor to acetonedicarboxylate complex and decomposition acetonedicarbox-ylate complex to manganese ferrite. There are endothermic (one) and exothermic (two) peaks corresponding to the citrate decomposition followed by manganese ferrite formation.

3.2. Dehydration of the citrate precursor

The amount of excess water depends on the atmospheric humidity and this amount varies from 4 to 10%. The extra water can be removed by heating the citrate precursor up to 100 °C that is shown by some weight loss in TG. Dehydration of the citrate precursor takes place between 115 and 135 °C with a maximum

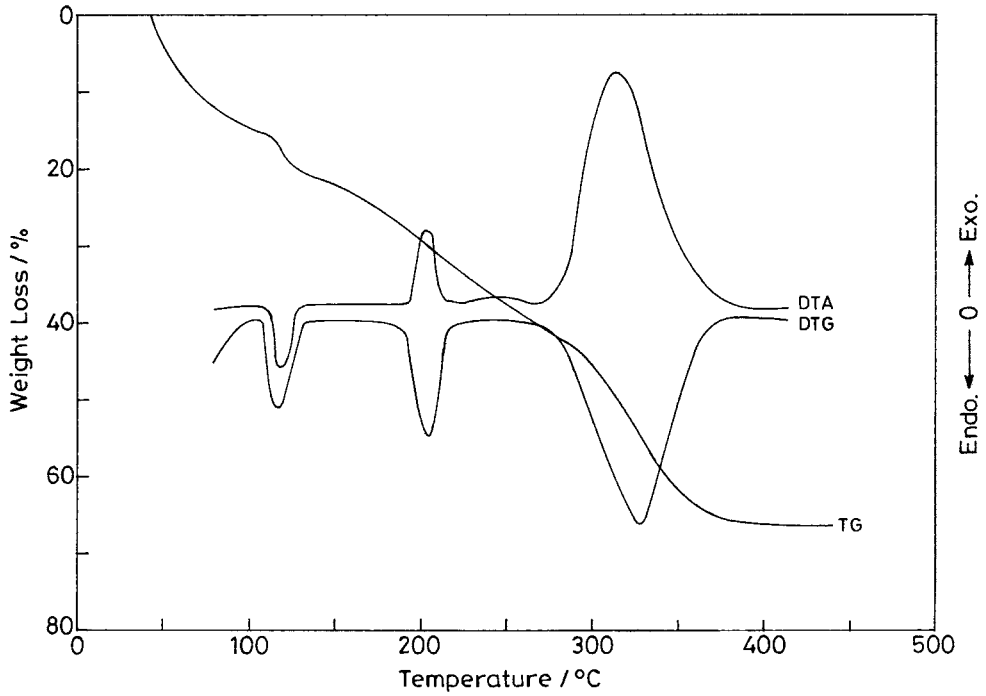

Fig. 1. (a) TG and (b) DTA curves recorded at the heating rate of 5 K min^{-1} for manganese iron citrate precursor.

around 120 °C. TG curve indicates a weight loss of 4.8% that agrees well with the calculated weight loss of 4.9% for the removal of six water molecules per mole of the citrate precursor. In the temperature range of 115–135 °C, we have observed an endothermic peak corresponding to the water removal. The temperature range mentioned above is valid only at a pressure of one atmosphere. The chemical analyses of anhydrous precursor result in Mn: 9.2%, Fe: 17.2% and citrate: 71.5%, which agree well with the calculated values of Mn: 7.9%, Fe: 16.0% and citrate: 76%. Static TG data is obtained by heating the precursor at different temperatures for 4 h duration time and is presented in Table 2.

3.3. Decomposition of the anhydrous precursor

Thermal decomposition of the anhydrous manganese iron citrate was found to be the most important and at the same time most complex stage of decomposition. The citrate precursor is probably converted to acetonedicarboxylate complex. This process is

Table 2
Weight loss in decomposition steps of $Mn_3Fe_6O_4(C_6H_6O_7)_8 \cdot 6H_2O$ recorded with varying rate

Steps	Temperature range (°C)	Static weight loss (%)	Dynamic weight loss (%)		
			Observed		Calculated
			5 K min^{-1}	10 K min^{-1}	
1	<100	12	4–10.0	4–10.0	–
2	115–135	5.3	4.8	5.1	4.9
3	170–230	13	11.0	11.0	10.7
4	200–320	37	40.3	40.1	52.8

found to be exothermic (Fig. 1) and large amounts of gases are evolved spontaneously. The decomposition of the anhydrous citrate precursor started around 170 °C and was accompanied by the evolution of CO gas. The weight loss of 11.0% was observed for the formation of acetonedicarboxylate complex $Mn_3Fe_6O_4(C_5H_6O_7)_8$ as shown in Table 2. There is an evolution of a large amount of CO gas and secondary reaction of carbon monoxide makes the process exothermic. At the end of this step a metastable acetonedicarboxylate complex was identified as the product. By isothermal heating of anhydrous manganese iron citrate in N_2 atmosphere around 220 °C for about 4 h, the acetonedicarboxylate was isolated. Evolved gas analysis (EGA) and TG weight loss indicates that 8.0 mol of CO gas was evolved. The calculated value for this step is 10.8%, which agree well with the observed data. Static weight loss data are also in good agreement with the dynamic TG data. The chemical analysis of the acetonedicarboxylate complex gave Mn: 9.5%, Fe: 18.3% and acetonedicarboxylate complex: 69.3% which are

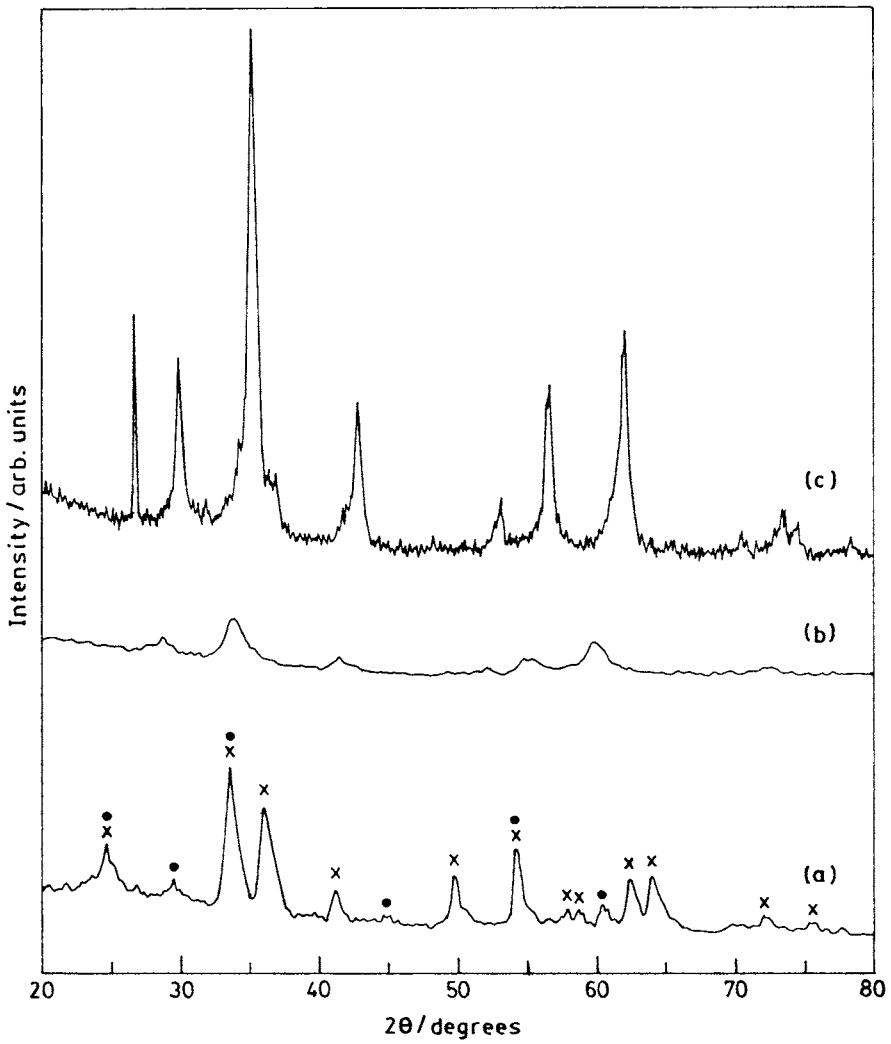

Fig. 2. XRD pattern of the final products when the precursor is (a) decomposed in air at 350 °C for 2 h (●) Mn_2O_3 and (×) Fe_2O_3 phases, (b) decomposed in N_2 at 330 °C for 4 h and (c) heated at 350 °C for 2 h in N_2 atmosphere.

comparable to the calculated values of Mn: 8.8%, Fe: 18.1% and acetonedicarboxylate: 73.1%. The acetonedicarboxylate complex was found to be X-ray amorphous.

3.4. Decomposition of acetonedicarboxylate complex

The acetonedicarboxylate complex started decomposing at around 300 °C in N_2 and the decomposition was complete at around 350 °C. At this stage the observed weight loss at 40.3% was found to be less than the calculated values than the calculated values of 52.8%. This may be due to the presence of carbon and/or adsorption of evolved gases on the ultrafine $MnFe_2O_4$ particles because of large surface area. The XRD pattern of thus obtained nanosize manganese ferrite particles showed a peak at 2θ value of 26.5 indicating the presence of carbon residue. The presence of carbon residue is understandable and is common during the decomposition of any organic molecules (excess citric acid and precursor), in the oxygen free atmosphere. At this stage, decomposition is a complex process that involves decarboxylation (i.e. evolution of CO_2) and acetone molecules are formed. The evolution of acetone was confirmed by heating the residue $Mn_3Fe_6O_4(C_6H_6O_7)_8$ in a cylindrical tube with flowing N_2 gas and condensing it in an ice cold $CDCl_3$. This evolved gas was trapped and analyzed by ^{1}H-NMR spectroscopy. The peak at $\delta = 2.2$ ppm confirmed the evolution of acetone during the decomposition process.

At higher temperature, i.e. above 300 °C, the citrate precursor structure collapses during decomposition and the formation of $MnFe_2O_4$ occurs with the evolution of acetone and CO_2 gas. Some reports are available [17,18] that have proposed the formation of a compound of the type $M_3Fe_6O_{12}(CO_2)_3$ (where M = Ni, Co) to explain the adsorption of CO_2 to explain the weight loss. Interestingly, the manganese ferrite is formed at much lower temperature, i.e. 350 °C, and the decomposition does not go through the formation of complex carbonates, as has been reported in the literature [22–24]. However, the heating rate was found to have no effect on the decomposition mechanism and weight loss. The corresponding temperatures corresponding to each step was found to shift to higher, nearly by 10 °C when the heating rate was 10 K min^{-1}.

3.5. X-ray diffraction, surface area measurements and electron microscopy studies

Fig. 2 shows XRD pattern for the final product after decomposition at 350 °C in air and in N_2 atmosphere. Fig. 2(a) shows pattern of the products of decomposition carried out in air. It is clear that spinel that is expected is not formed. This pattern matches well with two different phases of Mn_2O_3 (hausmannite) and α-Fe_2O_3 (haematite). These phases are marked appropriately in the figure. This is due to the oxidation of

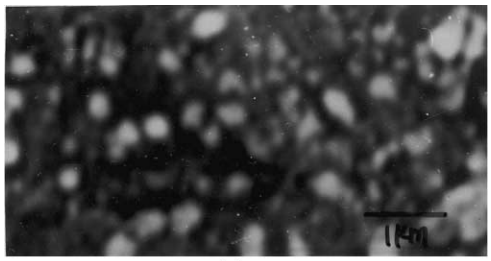

(a)

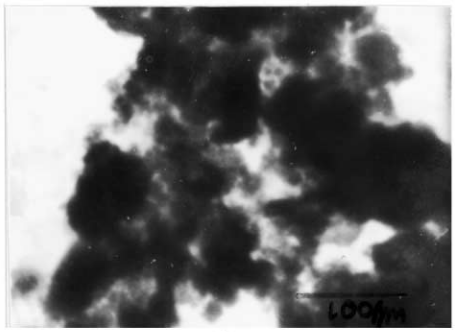

(b)

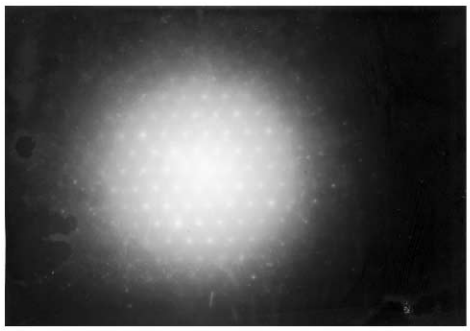

(c)

Fig. 3. (a) SEM micrograph, (b) TEM micrograph and (c) SAD pattern of the particles heat treated at 350 °C for 2 h in N_2 atmosphere.

Mn^{2+} to Mn^{3+} in the form of Mn_2O_3. The decomposition of manganese iron acetate pyridine complex salt in air up to 1000 °C, yields above phases [25]. The oxidation of Mn^{2+} starts at 200 °C in air and thus it is very difficult to obtain $MnFe_2O_4$ particles at relatively low temperatures [26]. Fig. 2(b) shows the broad peaks corresponding to the amorphous nature of the spinel phase when the precursor is heat treated at 330 °C for 4 h. Thus after the decomposition, manganese ferrite particles are directly formed without any intermediate phase. Fig. 2(c) shows clearly the formation of $MnFe_2O_4$ single phase when the citrate precursor decomposition was carried out in N_2 atmosphere at 350 °C for 2 h. XRD crystallite size was found to be 7.0 nm from the line broadening. Fig. 3 shows the SEM and TEM images and SAD pattern of these $MnFe_2O_4$ samples obtained at 400 °C. Electron microscopy study indicates the nanostructured nature and spherical morphology. Each particle exists as a monolith which diffracts coherently. The particle size distribution is almost uniform and these particles show agglomerates of 11 nm small crystallites. The crystallite size is found to be smaller than the respective particle size measured in SEM/TEM. The BET surface area is measured for the sample prepared at 350 °C and is found to be 98.0 $m^2\ g^{-1}$. The dimensions of the particle size calculated from the surface area are relatively larger than from XRD and microscopy. Thus, the formation of magnetic clusters or aggregates is confirmed.

3.6. Cation distribution study of nanosize $MnFe_2O_4$ particles by TG analysis

Fig. 4 shows the DTA studies carried out on nanosize $MnFe_2O_4$ particles formed at 350 °C. We have observed a small broad exothermic peak with a maximum at 380 °C when the $MnFe_2O_4$ nanoparticles are annealed during the thermal scans (Fig. 4(a)). TG of the same sample showed no weight loss. Thus, we predict that the peak in the DTA must be due to some structural changes accompanied by the heat change. To affirm these changes, the DTA of this annealed sample is once again recorded (Fig. 4(b)). The results show the absence of an exothermic peak that is accompanied with no weight loss observation. Therefore, we conclude that the structural change that occurs at 380 °C is irreversible. Thus, we propose that the heat change be due to the rearrangement of the ions in the $MnFe_2O_4$ lattice. The extent of occupancy

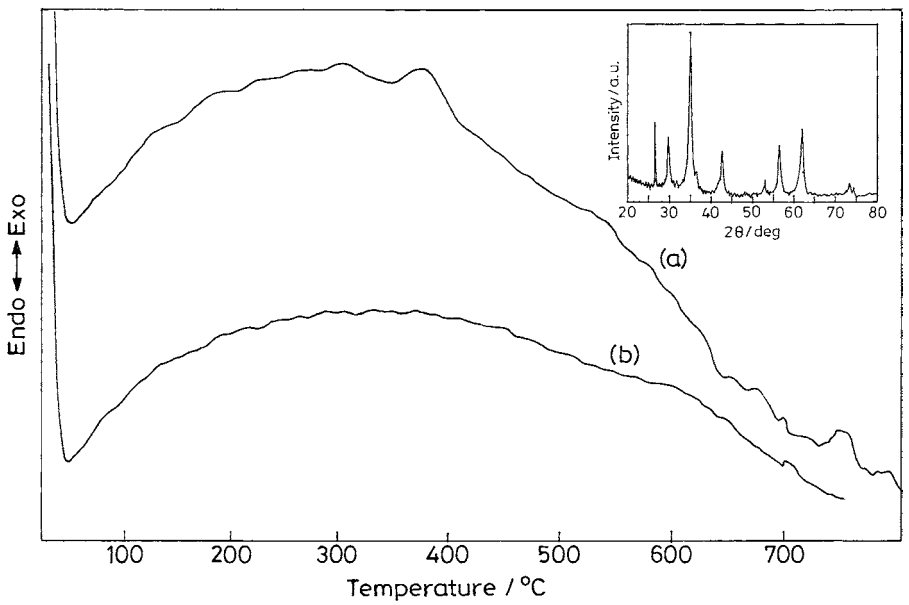

Fig. 4. (a) DTA of the $MnFe_2O_4$ particles prepared at 350 °C at rate of 5 K min^{-1} and (b) DTA of the $MnFe_2O_4$ particles annealed at 400 °C in (a) at the rate of 5 K min^{-1}. Inset figure shows the XRD pattern of this annealed sample.

of Mn^{2+} cations in the octahedral sites is termed as degree of inversion. Such a transition at around 400 °C has also been reported in the literature for the $MnFe_2O_4$ particles synthesized by co-precipitation technique [26,27]. The degree of inversion depends on the synthetic method employed. This degree of inversion changes to an equilibrium value after annealing at 400 °C. It is worth to point out that there is no change observed in the XRD pattern (Fig. 4, inset) and also in the particle size for the as prepared sample after the structural change. This implies that cubic spinel structure is maintained during the structural rearrangement. Thus, we infer that the rearrangement of Mn^{2+} cations occurs from the octahedral sites to tetrahedral sites and is accompanied by small heat change, which is an irreversible transition.

These nanocrystalline particles of $MnFe_2O_4$ exhibit superparamagnetic behavior in magnetic studies at room temperature and show magnetic ordering below the blocking temperature (75 K). The magnetic results are characteristic to the $MnFe_2O_4$ ferrite materials and are discussed in detail elsewhere [28].

4. Discussion

The literature contains scanty information on the use of citrate complexes for ferrite formation. However, thermal decomposition studies of citrate complex for the formation of garnets [29], and perovskite oxides [23,30–32] have been reported. These studies showed that citrate metal complex decomposition involves mainly three or four steps and the decomposition proceeds through intermediates such as aconitate, itaconate, itaconic anhydride and complex carbonates, leading to the respective oxides. In our laboratory, we have successfully studied and reported the formation of nanostructured garnets and ferrites [15,18]. The extent of polymerization to form a network of solid structures in the citrate complexes depends on pH and therefore manganese iron citrate precursor is obtained in the pH range 1.24–2.00. It was also was also difficult to predict the binding of metal ion sites with the citric acid. Therefore, plausible mechanism is proposed based on thermal analyses, gas analyses, XRD and IR data. Manganese iron citrate hexahydrate precursor decomposes to the $MnFe_2O_4$ phase in N_2 and the experimental results indicate following scheme:

1. $Mn_3Fe_6O_4(C_6H_6O_7)_8 \cdot (n+6)H_2O \underset{<100\,^\circ C}{\rightarrow} Mn_3Fe_6O_4(C_6H_6O_7)_8 \cdot 6H_2O + nH_2O$
2. $Mn_3Fe_6O_4(C_6H_6O_7)_8 \cdot 6H_2O \underset{115-135\,^\circ C}{\rightarrow} Mn_3Fe_6O_4(C_6H_6O_7)8 + 6H_2O$
3. $Mn_3Fe_6O_4(C_6H_6O_7)_8 \underset{170-230\,^\circ C}{\rightarrow} Mn_3Fe_6O_4(C_5H_6O_6)_8 + 8CO$
4. $Mn_3Fe_6O_4(C_5H_6O_6)_8 \underset{300-340\,^\circ C}{\rightarrow} 3MnFe_2O_4 + 8CH_3COCH_3 + 16CO_2$

Manganese iron citrate hexahydrate complex was isolated by removing extra adsorbed water at around 100 °C. The second step in the decomposition of the citrate precursor corresponds to the loss of coordinated water. During the third step there is an evolution of CO gas. The residue after this decomposition step has only a metastable composition $Mn_3Fe_6O_4(C_5H_6O_6)_8$. In the fourth step complete internal conversion of carboxylate groups, methylene groups and hydroxyl groups takes place to form acetone and CO_2 gas which can be observed by the disappearance of the absorption bands in the IR spectrum. Some carbon residue was also formed during the decomposition and ferrite particles are separated by carbon matrix. The actual reactions appear to be simpler in the second and third steps unlike the reactions proceeding through aconitate complex formation by analogy with the thermal decomposition through titanyl citrate complex [23]. Thus, we conclude that the decomposition does not proceed through the formation of complex carbonates and manganese ferrite is formed at a much lower temperature, i.e. 330 °C, which is an amorphous phase.

Thus, the $MnFe_2O_4$ particles synthesized by using the citrate precursor technique has a higher degree of inversion than that prepared by the normal ceramic technique. It is observed that degree of inversion depends on the inversion factor, thus it is possible to control this factor in order to achieve high performance. A peak at 380 °C in the DTA curve for the as prepared sample is attributed to the irreversible migration of Mn^{2+} from octahedral to tetrahedral sites. To corroborate this the DTA of the annealed sample already heated at temperatures around 400 °C showed no peak. The presence of even small amount of Mn^{3+} during synthesis will not lead to such a transition because of the fact that Mn^{3+} has higher affinity for octahedral coordination arising from the higher

crystal field stabilization energy (CFSE) [26]. In this experiment, we have demonstrated that our sample has no Mn^{3+} species. These observations were further confirmed by independent magnetic studies.

5. Conclusion

The synthesis of nanostructured $MnFe_2O_4$ ferrite by the citrate precursor method was investigated and the mechanism of thermal decomposition as examined in detail. The thermal decomposition of the citrate precursor in N_2 atmosphere proceeds through three major steps; dehydration, formation of acetonedicarboxylate complex, and decarboxylation process. Nanocrystalline $MnFe_2O_4$ particles having crystallite size of 7.0 nm are formed at 350 °C. Thus, $MnFe_2O_4$ particles synthesized by citrate precursor technique were found to have a higher degree of inversion compared to the materials prepared by normal ceramic technique. Thermal analysis studies also confirmed the rearrangement of Mn^{2+} from octahedral site to tetrahedral site that occurs irreversibly for as prepared samples at 380 °C and is associated with small heat change as an exothermic process.

Acknowledgements

We acknowledge financial assistance during this investigation by the Department of Science and Technology, New Delhi, India. One of us (NSG) wishes to thank Prof. H. Gleiter, Institute of Nanotechnology, Forschungszentrum Karlsruhe, for the encouragement during this investigation.

References

[1] J.L. Dormann, I. Fiorani (Eds.), Magnetic Properties of Fine Particles, North-Holland, Amsterdam, 1992.
[2] G.C. Hadjipanayis, R.W. Siegel (Eds.), Nanophase Materials: Synthesis—Properties—Applications, Kluwer Academic Publishers, Boston, 1993.
[3] A.S. Edelstein, R.C. Cammarata (Eds.), Nanomaterials: Synthesis, Properties and Applications, Institute of Physics, Bristol, 1996.
[4] C.B. Murray, C.R. Kagan, M.G. Bawendi, Science 270 (1995) 1335.
[5] A.P. Alivisators, Science 271 (1996) 933.
[6] D. Davidovik, M. Tinkham, Appl. Phys. Lett. 73 (1998) 3959.
[7] S.H. Charap, P.L. Lu, Y. He, IEEE Trans. Magn. 33 (1997) 978.
[8] R.P. Andres, et al., Science 272 (1996) 1323.
[9] V.A.M. Brabers, in: K.H.J. Buschow (Ed.), Handbook of Magnetic Materials, Vol. 8, Elsevier, Amsterdam, 1995.
[10] S. Komarneni, E. Fregeau, E. Breval, R. Roy, J. Am. Ceram. Soc. Commun. C 71 (1988) 26.
[11] A.H. Morrish, K. Haneda, J. Appl. Phys. 52 (1981) 2696.
[12] D.W. Johnson Jr., Am. Ceram. Soc. Bull. 60 (1981) 221.
[13] C.H. Marcilly, P. Courty, B. Delmon, J. Am. Ceram. Soc. 53 (1970) 56.
[14] Z.X. Tang, C.M. Sorenson, K.J. Klabunde, G.C. Hadjipanayis, J. Colloid. Interf. Sci. 148 (1991) 38.
[15] V.K. Shankaranarayanan, N.S. Gajbhiye, Thermochim. Acta 153 (1989) 337.
[16] V.K. Shankaranarayanan, N.S. Gajbhiye, J. Am. Ceram. Soc. 73 (1990) 1301.
[17] N.S. Gajbhiye, S. Prasad, Thermichim. Acta 285 (1996) 325.
[18] S. Prasad, A. Vijayalakshmi, N.S. Gajbhiye, J. Therm. Anal. 52 (1998) 595.
[19] D.G. Wickham, E.R. Whipple, E.G. Larson, J. Inorg. Nucl. Chem. 14 (1960) 217.
[20] A.I. Vogel, Text Book of Quantitative Analysis, ELBS, England, 1986.
[21] O.N. Karpov, Tr. Vses Nauchin.-Issled Inst. Khim. Reaktivov 25 (1963) 334.
[22] H.S. Gopalakrishnamurthy, M. Subbarao, T.R.N. Kutty, J. Inorg. Nucl. Chem. 37 (1975) 891.
[23] D. Hennings, W. Mayr, J. Solid State Chem. 26 (1978) 329.
[24] N.S. Gajbhiye, U. Bhattacharya, V.S. Darshane, Thermochim. Acta 264 (1995) 219.
[25] D.G. Wickham, Inorg. Synth. 8 (1962) 152.
[26] J.P. Chen, C.M. Sorenson, K.J. Klabunde, G.C. Hadjipanayis, E. Devlin, A. Kostikas, Phys. Rev. B 54 (1996) 9288.
[27] Z. Simsa, V.A.M. Brabers, IEEE Trans. Mag 11 (1975) 1303.
[28] N.S. Gajbhiye, G. Balaji, Phys. Stat. Solidi, in press.
[29] T.J.A. Popma, V. Diepen, Mater. Res. Bull. 9 (1974) 111.
[30] J.M.D. Tascon, S. Mendioroz, L. Gonzalez Tejuca, Z. Phys. Chem. Neue. Fol. 124 (1981) 109.
[31] H.M. Zhang, Y. Teraoka, N. Yamazoe, Chem. Lett. 4 (1987) 665.
[32] D.J. Anderton, F.R. Sale, Powder Metall. 22 (1979) 14.